

LA-UR-01-0352

Approved for public release;
distribution is unlimited.

Title:

Helioseismic tests of the new Los Alamos LEDCOP opacities

Author(s):

C. Neuforge-Verheecke, J.A. Guzik, J.J. Keady, N.H. Magee, P.A. Bradley, A. Noels

Submitted to:

<http://lib-www.lanl.gov/la-pubs/00367077.pdf>

Los Alamos National Laboratory, an affirmative action/equal opportunity employer, is operated by the University of California for the U.S. Department of Energy under contract W-7405-ENG-36. By acceptance of this article, the publisher recognizes that the U.S. Government retains a nonexclusive, royalty-free license to publish or reproduce the published form of this contribution, or to allow others to do so, for U.S. Government purposes. Los Alamos National Laboratory requests that the publisher identify this article as work performed under the auspices of the U.S. Department of Energy. Los Alamos National Laboratory strongly supports academic freedom and a researcher's right to publish; as an institution, however, the Laboratory does not endorse the viewpoint of a publication or guarantee its technical correctness.

Helioseismic tests of the new Los Alamos LEDCOP opacities

C. Neuforge-Verheecke^{1,4}, J.A. Guzik¹, J.J. Keady², N.H. Magee², P.A. Bradley¹, A. Noels³

¹*Applied Physics Division, Los Alamos National Laboratory, X-2, MS B220, Los Alamos, NM 87545, USA*

²*Theoretical Division, Los Alamos National Laboratory, T-4, MS B212, Los Alamos, NM 87545, USA*

³*Institute of Astrophysics and Geophysics, University of Liège, 5 avenue de Cointe, 4000 Liège, Belgium*

ABSTRACT

We compare the helioseismic properties of two solar models, one calibrated with the OPAL opacities and the other with the recent Los Alamos LEDCOP opacities. We show that, in the radiative interior of the Sun, the small differences between the two sets of opacities (up to 6% near the base of the convection zone) lead to noticeable differences in the solar structure (up to 0.4% in sound speed), with the OPAL model being the closest to the helioseismic data. More than half of the difference between the two opacity sets results from the interpolation scheme and from the relatively widely spaced temperature grids used in the tables. The remaining 3% intrinsic difference between the OPAL and the LEDCOP opacities in the radiative interior of the Sun is well within the error bars on the opacity calculations resulting from the uncertainties on the physics. We conclude that the OPAL and LEDCOP opacity sets do about as well in the radiative interior of the Sun.

Subject headings: – Sun: interior – Sun: helioseismology

1. Introduction

Opacities are a key ingredient in stellar evolution and pulsation calculations. Recently, a new set of Los Alamos opacities has been computed, using an updated version of the Los

⁴Present address: Institute of Astrophysics and Geophysics, University of Liège, 5 avenue de Cointe, 4000 Liège, Belgium

Alamos LEDCOP (Light Element Detailed Configuration Opacity) code (Magee et al. 1995; <http://www.t4.lanl.gov>)

In this paper, we compare two solar models calibrated with the OPAL opacities (Iglesias & Rogers, 1996) and the recent Los Alamos opacities, in light of the current helioseismic data.

The paper is organized as follows: In section 2, we present the evolution modeling and input physics. Our calibrated models are discussed and confronted with helioseismic observations in Sect. 3. We discuss the possible origin of the differences between the OPAL and the LEDCOP opacities in Sect. 4 and we present our conclusions in Sect. 5.

2. Evolution modeling and input physics

We evolved our solar models using an extensively updated version of the Iben code (1963, 1965a, 1965b). Our code is described in Guzik & Swenson (1997) and in Neuforge et al. (2001). It includes the treatment of Burgers (1969) to calculate the thermal, gravitational and chemical diffusion of the electrons, ^1H , ^3He , ^4He , ^{12}C , ^{14}N , ^{16}O , ^{18}O , ^{20}Ne , and ^{24}Mg (see Cox et al. (1989) for details). Our convection treatment is the standard mixing length theory (Cox & Giuli 1968), together with the Schwarzschild criterion for convective stability. Our models do not contain convective overshoot or mixing in the tachocline. We adopted the SIREFF analytical equation of state (Guzik & Swenson (1997) and the the solar mixture of Grevesse and Noels (1993, GN93). All charged-particle induced reactions rates are taken from of Angulo et al. (1999), whereas the ^7Be electron capture rate is taken from Adelberger et al. (1998). We use Salpeter's weak screening formula (see e.g., Clayton 1983) to evaluate the effect of electrostatic screening, as prescribed in Gruzinov & Bahcall (1998). The opacity tables that we use in the solar interior (either OPAL or LEDCOP) are connected to the low-temperature opacities of Alexander and Ferguson (1995, private communication) by a sinusoidal temperature average between 7500K and 9500K.

3. Model calibrations and helioseismic comparisons

We use a standard procedure to calibrate our models: we adjust the initial helium abundance Y_0 , the initial metallicity Z_0 , and the mixing length to pressure scale height ratio α , to match the solar radius R_\odot , the solar luminosity L_\odot , and the present surface Z/X abundance at the present solar age t . The mass of our models is $1.9891 \times 10^{33}\text{g}$ (Cohen & Taylor 1986). We adopted $R_\odot = 6.9599 \times 10^{10} \text{ cm}$, $L_\odot = 3.846 \times 10^{33} \text{ erg s}^{-1}$, and $t = 4.52$

Gyr, (see Guenther et al., 1992 and references therein). We use the value $Z/X = 0.0245$ from the GN93 mixture.

Our evolution models have ~ 450 zones and are evolved for ~ 500 time-steps from a homogeneous pre-main sequence model. The zero-age main sequence model is defined as the model of minimum radius.

The characteristics of our calibrated models are presented in Table 1. The OPAL model corresponds to Model 1 of Neuforge et al. (2001), whereas the LEDCOP model has been calculated using the recent Los Alamos opacities.

Only the OPAL model has a convection zone base location (see Table 1) in agreement with the helioseismic inferences of Basu (1997): $R/R_\odot = 0.713 \pm 0.001$. The convection zone of the LEDCOP model is too shallow ($R/R_\odot = 0.718$), due to the fact that the Los Alamos opacities are up to 6 % lower than the OPAL opacities near the base of the convection zone, as can be seen from Figure 1.

The discrepancies between the two sets of opacities also appear in the sound speed distribution of our two models. Figure 2 illustrates the relative differences in temperature and sound speed between the two models, as a function of the fractional radius.

The sound speed differences between the OPAL and the LEDCOP model can be understood the following way. Most of the solar convection zone is adiabatic. As a result, the structure of the convection zone is determined by the equation of state, the composition, and the (constant) specific entropy: a change of opacity has no effect. Small differences in composition and temperature between the OPAL and the LEDCOP model result from differences in the OPAL and LEDCOP opacities in the radiative interior and the calibration procedure (see below), but these differences cancel out and leave the sound speed unaffected. In the radiative interior, the squared sound speed behaves like T/μ , where T is the temperature and μ the mean molecular weight. The temperature differences between the two models follow the opacity differences: from the base of the convection zone to the center, the temperature gradient is proportional to the opacity. The initial hydrogen and heavy element abundances are slightly higher in the LEDCOP model than in the OPAL model. This adjustment is required to obtain a model with the correct luminosity and compensates for the lower LEDCOP opacities in most of the radiative interior of the model. The net effect is that the initial mean molecular weight is lower (0.6115) in the LEDCOP model than in the OPAL model (0.6125). It remains so in the course of the evolution. Near the center, the LEDCOP opacities are higher than the OPAL ones. However, the differences are too small to increase sufficiently the central temperature distribution of the LEDCOP model with respect to the OPAL one and make the LEDCOP model burn its hydrogen more

efficiently than the OPAL model.

The temperature differences dominate or go in the same direction as the mean molecular weight differences ($(\mu_{OPAL} - \mu_{LEDCOP} / \mu_{OPAL}) \simeq 0.16\%$). The net result is that the sound speed differences between the two models essentially follow the trend of the temperature differences (see Figure 2), and thus the trend of the opacity differences (see Figure 1).

Figure 3 shows a comparison between the sound speed in our models and Basu et al. (2000) seismic inversion. The agreement is better for the OPAL model, from the base of the convection zone to $R/R_\odot = 0.12$, because it has higher opacities than the LEDCOP model in this region. Higher opacities imply a higher temperature and thus a higher sound speed. As a result, the relative sound speed differences between our models and the seismic inversion of Basu et al. (2000) are lower. From $R/R_\odot = 0.12$ to 0.07 (the limit of the inversion), the LEDCOP model does a better job because it has higher opacities than the OPAL model in this region. From the center to $R/R_\odot = 0.15$, the differences in opacities amount to less than 2.5% and have too small an effect on the temperature profile to significantly affect the neutrino predictions.

The direct frequency comparisons confirm the sound speed comparisons. We use the non-adiabatic pulsation code of Pesnell (1990) to calculate the p-mode oscillation spectrum of our models. For the low-degree frequency comparisons ($\ell = 0, 1, 2, 3$), we use a hybrid set of observational data chosen to maximize the number of observed low-degree modes in the set and minimize the observational uncertainties. This set is fully described in Neuforge et al. (2001). For the intermediate degree frequency comparisons, we use the data from Schou & Tomczyk (1996). Figure 4 shows observed minus calculated nonadiabatic frequency differences (in μHz) vs. calculated frequency (in μHz) for low ($\ell = 0, 1, 2$ and 3) and intermediate-degree ($\ell = 5, 10, 15$ and 20) p-modes from our calibrated models. The agreement is better for the OPAL model. The reasons for the trends in frequency differences have been investigated. The upward trend in O-C frequency at low frequency can be removed by decreasing the adopted value for the present solar radius by about 400 km, as was recently derived by Brown & Christensen-Dalsgaard (1998). The downward trend can be removed by a very slight adjustment to the sound speed gradient at the top of the solar convection zone, between 9,000 and 12,000 K. All of these modes pass through this region of the Sun, but are more or less sensitive to it depending on the shape of the eigenfunction in this region. Models with improved treatments of convection that include, for example, turbulent pressure effects, can remove this trend. The overall upward or downward shift in O-C frequency for these low and intermediate-degree modes, however, can be adjusted by changing the depth of the convection zone. The O-C frequencies of the LEDCOP model are generally higher than those of the OPAL model because the convection zone is shallower, and further from the optimum value of $0.713 R_\odot$ inferred from helioseismology. Moreover, the

dispersion in frequency difference as a function of degree is larger for the LEDCOP model, the modes of different ℓ being affected differently by the opacity differences between the two models. This occurs because modes of different ℓ have different lower turning points and are therefore sensitive to different integrated regions of the Sun from the surface to the turning point.

The small structural differences in the central regions do not affect significantly the small frequency separations, as can be seen from Figure 5.

4. Comments on the Opacity Differences

The OPAL and LEDCOP opacities differ by $\sim 6\%$ at the base of the convection zone. We have examined the LEDCOP opacity tables in detail to understand where the differences might originate and what can be done to reduce the discrepancy in future comparisons. There appear to be three causes for the differences: the opacity models, the interpolation methods, and the resolution of the temperature grids used by the two tables.

Little information about the opacity models can be extracted from the astrophysical opacity tables, since they contain a mixture of almost 30 elements, which has been integrated over frequency and then has been interpolated in R ($=\rho/(T/10^6)^3$). At the latest opacity workshop, (Rose, 2001), the opacities for the GN93 mixture at the center of the Sun were compared, with the OPAL results 3 % higher than LEDCOP. There are no comparisons at the exact physical conditions of the convection zone base ($\log T = 6.34$, $\log R = -1.75$), but some pure element cases (Rickert et al., 1995), mainly iron and carbon, are relatively close to these physical conditions ($\log T = 6.30$, $\log R = -1.50$). Concentrating principally on iron and taking into account the relative contributions to the mixture from the individual elements, we estimate that the LEDCOP opacities intrinsically are $2.5 \pm 2\%$ lower than OPAL for this (T, R) regime.

The pure element LEDCOP opacities are calculated on a temperature (T) and chemical potential grid, which allows the elements to be combined into mixtures. This table is then linearly interpolated in density to the final T-R astrophysical table grid. A spline interpolation is then used to obtain opacities for all X , Z , T and R . The spline interpolation has been checked and is able to reproduce the tabular values to within $\sim 1\%$. When the interpolated opacity at the convection zone base was compared with a direct opacity calculation by LEDCOP, the interpolated value was 3.5 % lower than the actual calculation, with an uncertainty of 1 % due to the spline interpolation. Independent comparisons for oxygen confirm that the linear interpolation routines produce values that are 4 to 5 % low for oxygen in this region

of the T-R table.

A final source of discrepancy is due to the different logarithmic temperature grids used by OPAL and LEDCOP. Each table has 10 temperatures per decade, but with different spacing. The LEDCOP table does not have an opacity value near $\text{LogT} = 6.30$ and $\text{logR} = -1.5$, whereas the OPAL table does. This point is an inflection point in the opacity curve and without this point for the spline interpolation, the interpolated opacity at the base of the convection zone will be too low by $1.5 \pm 0.5 \%$.

In summary, more than half of the opacity difference between OPAL and LEDCOP at the base of the convection zone is due to interpolation errors and the choice of the temperature grid: $(3.5 \pm 1 \%) + (1.5 \pm 0.5 \%) = (5. \pm 1.5 \%)$. Both of these problems can be reduced or eliminated by calculating more grid points for the original elemental calculations and using this finer mesh to produce astrophysical tables with more temperatures and at least twice as many R curves. There is still a fundamental difference of 2.5 to 3 % between the OPAL and LEDCOP opacities. We believe that this is due to differences in line transition energies, different level abundances obtained by the two equations of state, continuum lowering models, and treatment of far line wings, especially for the H-like and He-like Stark profiles.

Over the past 12 years, there have been a series of opacity workshops (see e.g. Rickert et al., 1995, Serduke et al., 2000 and references therein), in which OPAL, LEDCOP and many other opacity codes have been compared in detail. These numerous code comparisons showed that the opacities can vary by a few percent due to slight modifications in the choice of the physics used in the codes. These comparisons include pure elements, and some simple mixtures in the density-temperature range of interest to the solar interior. For pure Fe, OPAL and LEDCOP Rosselands are typically within 5-15 %, with occasional larger excursions, typically (though not always) in the strongly coupled plasma regime. Excluding the strongly coupled plasma regime, (not relevant for our discussion), for the remaining six (non-astrophysical) mixtures (which were calculated by both codes at precisely the same density-temperature points), the scatter in the in the mixture Rosselands ranges from 1-12 %. In code comparisons involving binary mixtures, ternary mixtures, ..., (where all components have significant abundance) it is sometimes noticed that the code agreement in the mixture opacities is somewhat better than the agreement of the constituent opacities. This is probably because, for a harmonic mean, the strong overlapping absorption fills in many of the deep valleys contributing the most to the given uncertainty for any one element. The upshot is that while the scatter in the Rosseland mean opacity for the the mixture is somewhat less than for the pure elements, it is reasonable to admit an error bar of at least 5 % on the opacity calculations due to the uncertainties affecting the physics currently used

in the codes. The fundamental difference between the OPAL and LEDCOP opacities is well within this margin of error. Therefore, we have confidence in the LEDCOP calculations. Nevertheless, the origin of this fundamental difference cannot be fully resolved until the next opacity workshop, at the earliest.

We also need to stress that even if direct code comparisons can increase confidence, it is less certain how to quantify the absolute uncertainty. Even though two codes may agree to within a certain amount, in the absence of experimental data it is unknown whether the correct result lies between the two calculations, or is significantly above or below both calculations. The most direct way to quantify the uncertainty in opacity calculations is a direct experimental spectral measurement of the transmission of a well characterized radiation source through a uniform (density and temperature) plasma sample. For the physical conditions starting at the base of the solar convection zone and heading inward, there are no direct opacity measurements. For conditions just below the base of the convection zone, hydrogenic oxygen is an important opacity contributor, and M-shell absorption of iron (and iron peak elements) is still contributing, while the L-shell absorption has also become important. Quantitative measurements of iron M-shell absorption at lower temperatures and densities; $\log T = 5.37$ and $\log R = -2.1$ (Springer et al., 1997), and $\log T = 5.84$ and $\log R = -1.4$ (Springer et al., 1992), exist. Calculated Rosseland means agree to within $\sim 10\%$ with experimentally determined Rosseland means (integrated over the experimental bandpass). Detailed comparison of the calculated and experimental monochromatic transmissions reveals a wealth of additional information, indicating that the good agreement of the means is far from accidental, and provides similar confidence about the calculation of M-shell absorption at other temperatures and densities.

5. Conclusions

We calibrated two solar models using the OPAL opacities Iglesias & Rogers (1996) and the recent Los Alamos LEDCOP opacities. The OPAL opacities are a few percent higher than the Los Alamos opacities in most of the radiative interior of the Sun, with the largest differences occurring near the base of the convection zone. As a consequence, the model calibrated with the OPAL opacities agrees better with the helioseismic constraints (sound speed distribution, location of the base of the convection zone, and direct frequency comparisons) than the model calibrated using the Los Alamos opacities. However, more than half the discrepancies between the two opacity sets can be attributed to interpolation errors and to the temperature grid choice. The remaining fundamental difference of 2.5 to 3 % between the OPAL and the LEDCOP opacities in the radiative interior of the Sun is

well within the error bars on the opacity calculations resulting from the uncertainties on the physics used in the codes. For these reasons, we can conclude that both opacity sets produce models that reproduce equally well the current helioseismic constraints.

This work was supported by NASA Astrophysics Theory Program grant S-30934-F and by SSTC grant (Pôle d'Attraction Interuniversitaire) P4/05 (Belgium). It has made use of the NASA's Astrophysics Data System Abstract Service and of the OPAL Web site, http://www-phys.llnl.gov/V_Div/OPAL/ to generate opacity tables. We are grateful to Carlos Iglesias for providing us with results in advance of publication.

REFERENCES

Adelberger, E.G., et al. 1998, *Rev. Mod. Phys.*, 70 (4), 1265

Angulo, C., et al. 1999, *Nuclear Physics*, A656, 3

Bahcall, J.N., & Ulrich, R.K. 1988, *Rev. Mod. Phys.*, 60 (2), 297

Bahcall, J.N., et al. 1996, *Phys. Rev.*, C54, 411

Bahcall, J.N. 1997, *Phys. Rev.*, C56, 3391

Basu, S. 1997, in *Sounding Solar and Stellar Interiors*, IAU Symp. 181, ed. J. Provost, & F.X. Schmider (Dordrecht: Kluwer Academic Publishers), 137

Basu, S., Bahcall, J.N., & Pinsonneault, M.H. 2000, *ApJ*, 529, 1084

Brown, T.M. & Christensen-Dalsgaard, J. 1998, *ApJ*, 500, L195

Burgers, J.M. 1969, *Flow Equations for Composite Gases* (New York: Academic)

Clayton, D.D. 1983, *Principles of Stellar Evolution and Nucleosynthesis* (Chicago: The University of Chicago Press)

Cohen, E.R., & Taylor, B.N. 1986, in *Codata Bulletin* 63, ed. National Bureau of Standards, p. 1

Cox, J.P., & Giuli, R.T. 1968, *Principles of Stellar Structure* (New York: Gordon and Breach)

Cox, A.N., Guzik, J.A., & Kidman, R.B. 1989, *ApJ*, 342, 1187

Grevesse, N., & Noels, A. 1993, in *Origin and Evolution of the Elements*, ed. N. Prantzos, E. Vangioni-Flam, & M. Cassé (Cambridge: Cambridge Univ. Press), p. 15 (GN93)

Gruzinov, A.V., & Bahcall, J.N. 1998, *ApJ*, 504, 996

Guenther, D.B., Demarque, P., Kim, Y.C., & Pinsonneault, M.H. 1992, *ApJ*, 387, 372

Guzik, J.A., & Swenson, F.J. 1997, *ApJ*, 491, 967

Iben, I. 1963, *ApJ*, 138, 452

Iben, I. 1965a, *ApJ*, 141, 993

Iben, I. 1965b, *ApJ*, 142, 421

Iglesias, J.A., & Rogers, F.J. 1996, ApJ, 464, 943

Magee, N. H., Abdallah, J., Jr., Clark, R. E. H., Cohen, J. S., Collins, L. A., Csanak, G., Fontes, C. J., Gauger, A., Keady, J. J., Kilcrease, D. P.& Merts, A. L. 1995, in proceedings of Joint Discussion No. 16 of the 22nd. General IAU Assembly, “Astrophysical Applications of Powerful New Databases”, ASP Conference Series, 78 ed. S.J. Adelman & W.L. Wiese (Astronomical Society of the Pacific, San Francisco, California), p. 51.

Neuforge, C., Goriely, S., Guzik, J.A., Bradley, P.A. & Swenson, F.J. 2001, ApJ, 550, 493

Pesnell, W.D. 1990, ApJ, 363, 227

Rickert, A. 1995, JQSRT, 54, 325

Rose, S. J. 2001, JQSRT, in press

Schou, J., & Tomczyk S. 1996, m2 table,
[http://www.hao.ucar.edu/public/research
/mlso/LowL/data.html](http://www.hao.ucar.edu/public/research/mlso/LowL/data.html)

Serduke, F.J., Minguez,E., Davidson, S.J., Iglesias, C.A., JSQRT, 65, 527

Springer, P.T. et. al. 1997, JQSRT, 58, 927

Springer, P.T. et. al. 1992, AIP Conference Proceedings 257, “Atomic Processes in Plasmas”, eds. E.S. Marmar and J.L. Terry, AIP, New York, 78

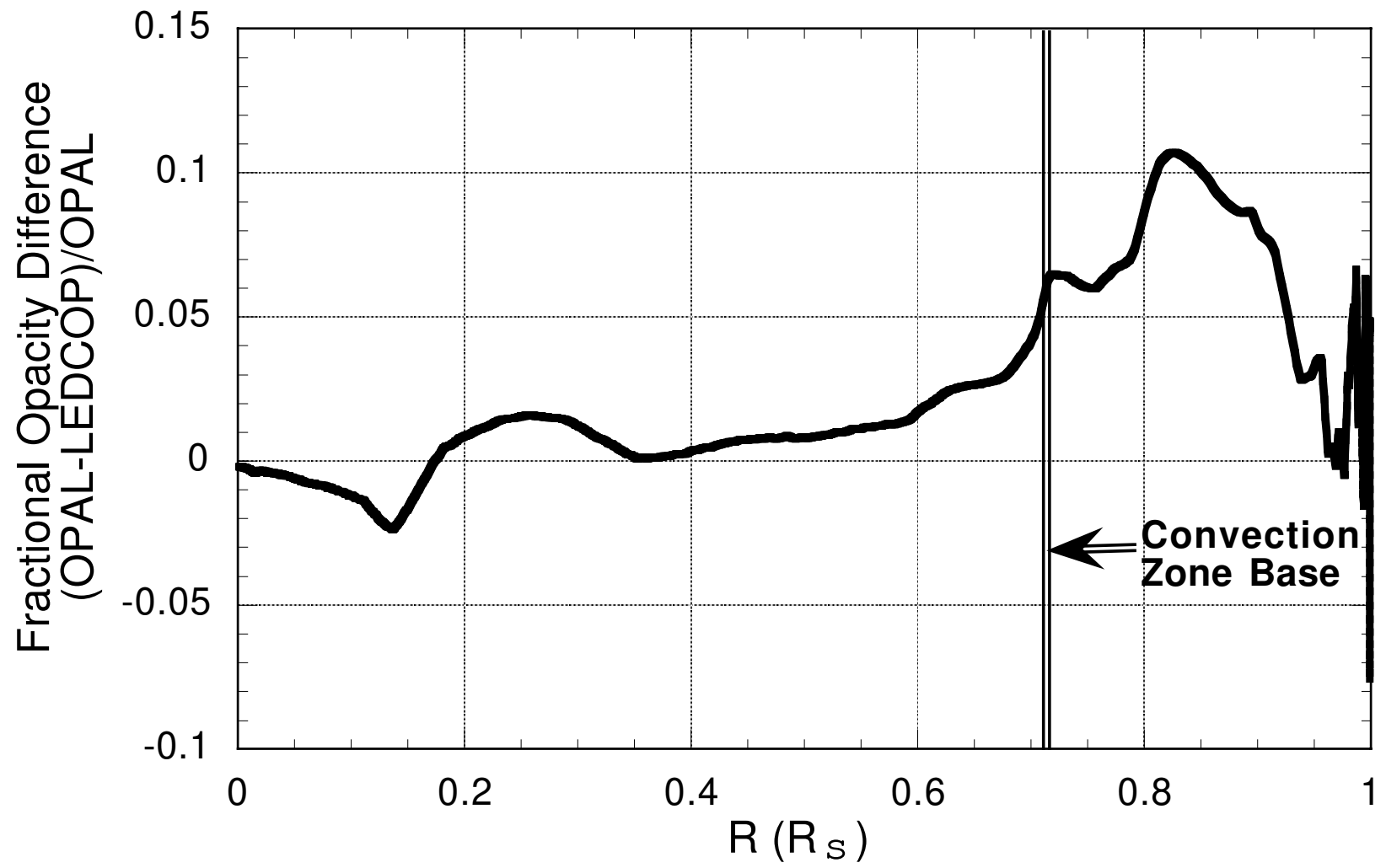
Fig. 1.— Relative differences (in %) between the OPAL and the Los Alamos opacities, as a function of the fractional radius.

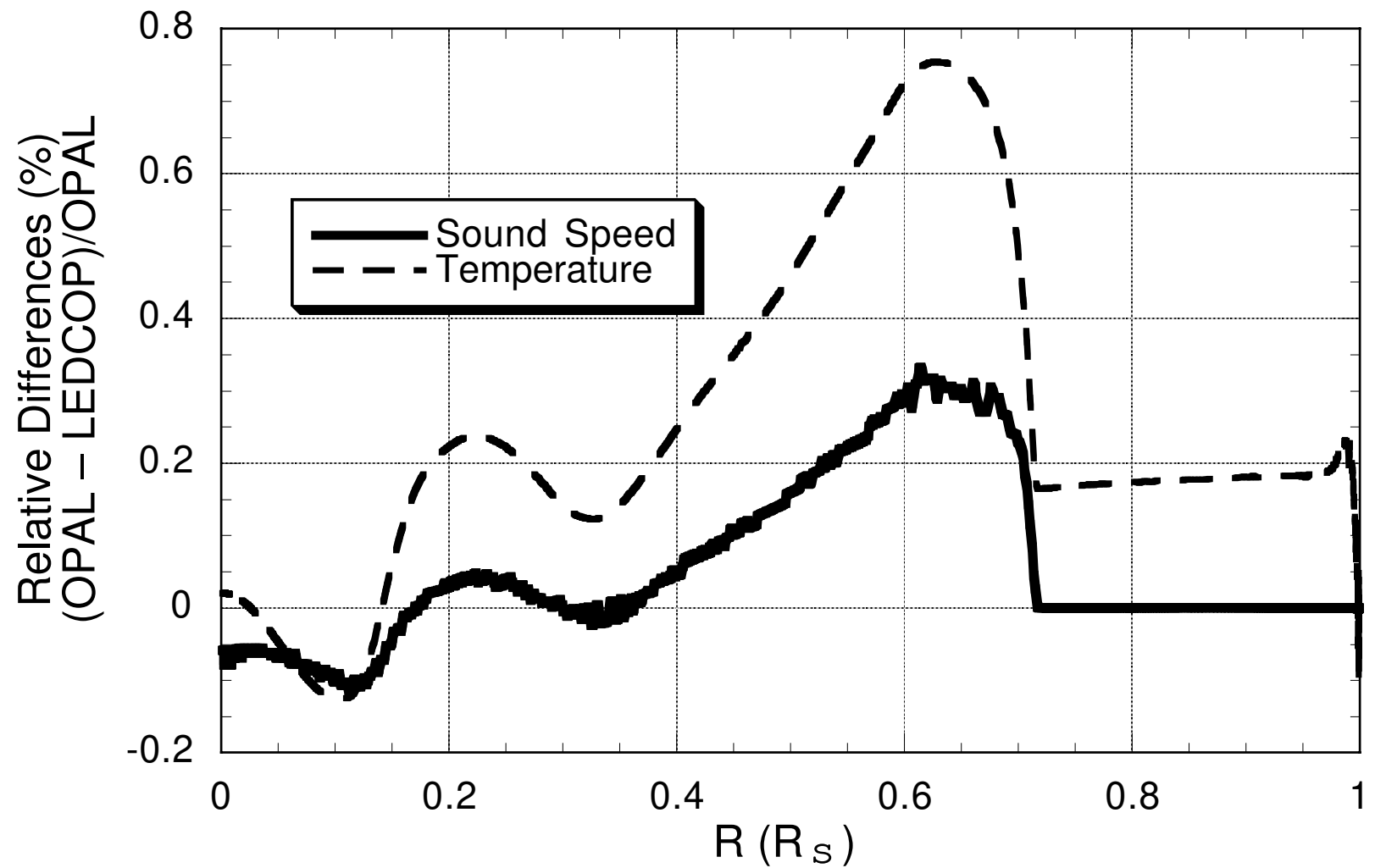
Fig. 2.— Relative temperature and sound speed differences (in %) between our models, as a function of the fractional radius.

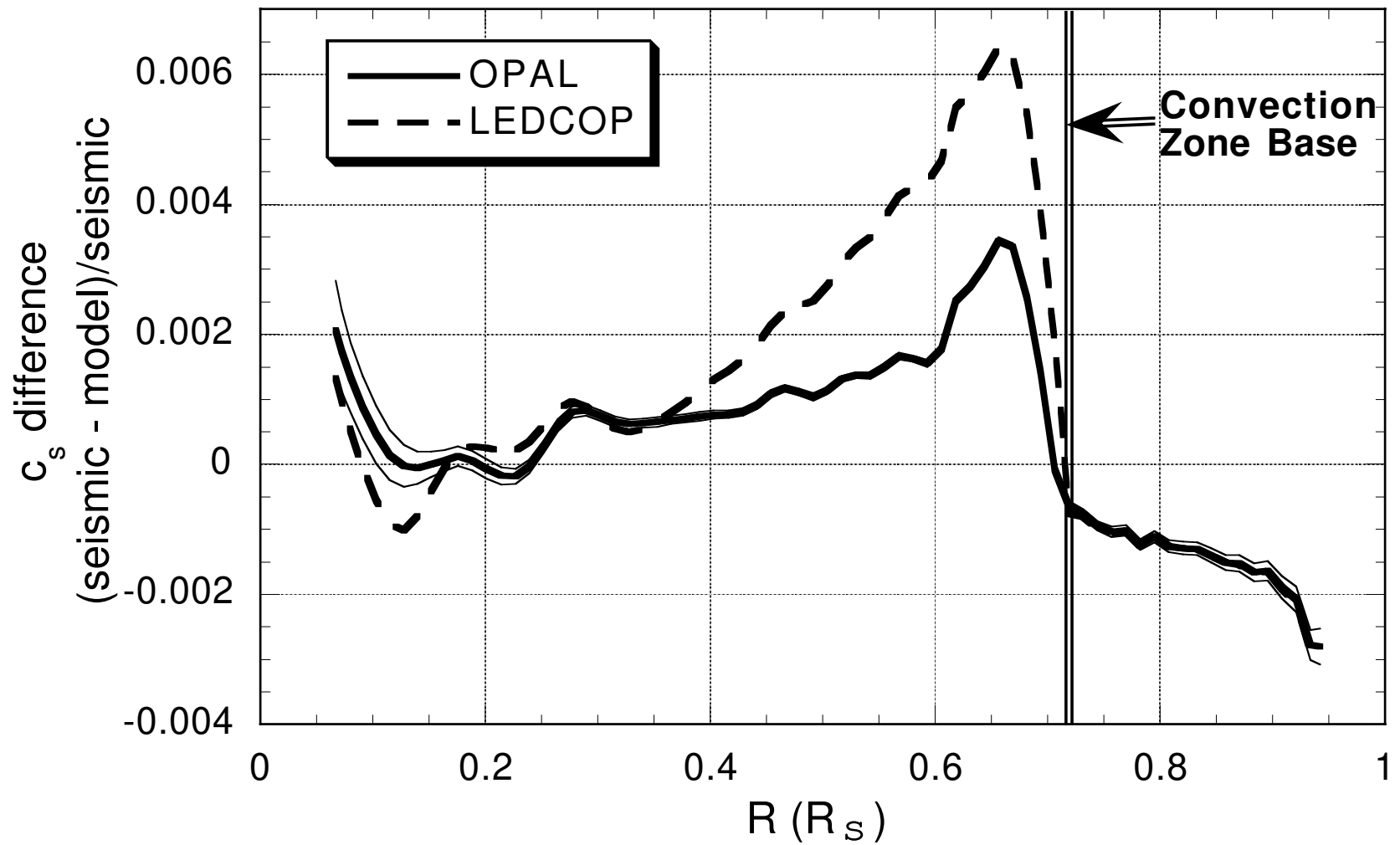
Fig. 3.— Relative sound speed differences between our models and the seismic inversion of Basu et al. (2000), $(c_{seismic} - c_{model})/c_{seismic}$, as a function of the fractional radius.

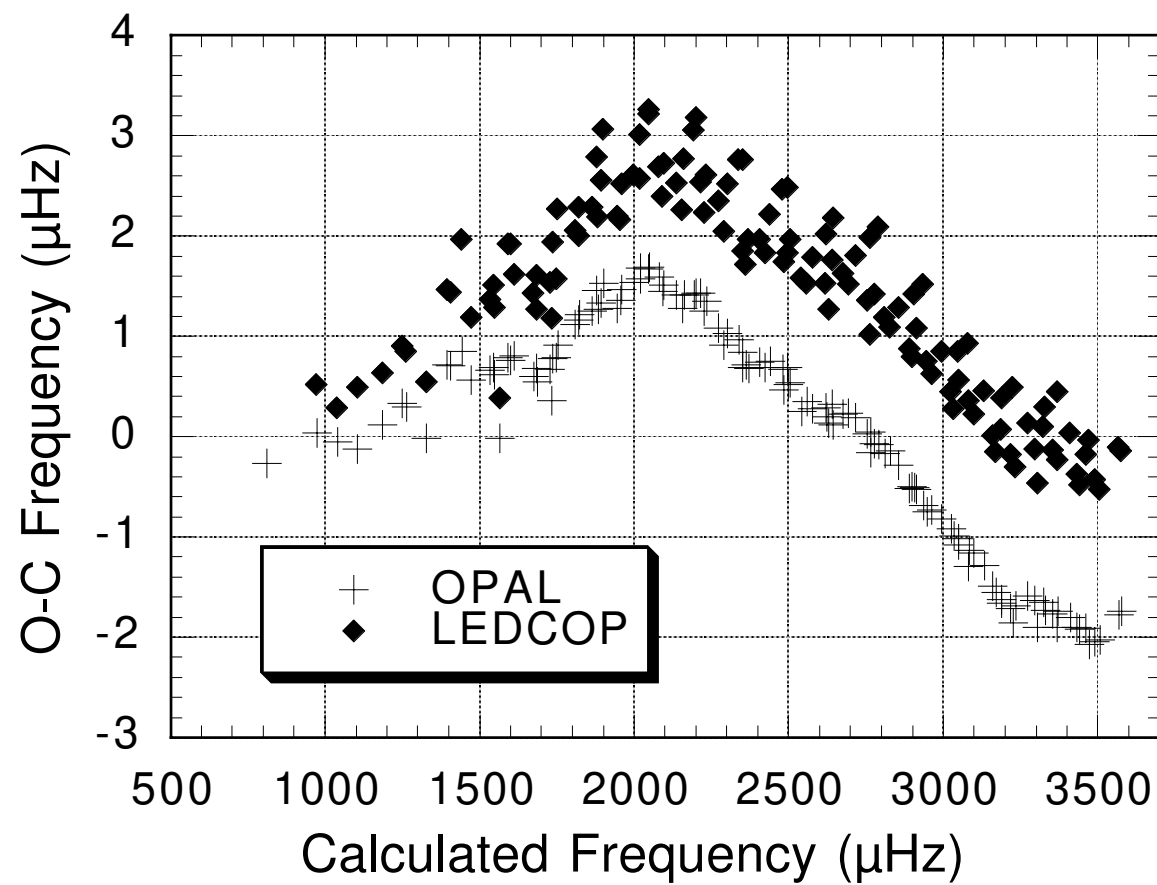
Fig. 4.— (O-C) nonadiabatic frequency differences (in μ Hz) vs. calculated frequency (in μ Hz) for low ($\ell = 0, 1, 2$ and 3) and intermediate-degree ($\ell = 5, 10, 15$ and 20) p-modes from our calibrated models.

Fig. 5.— Small frequency separations ($\nu_{0,n} - \nu_{2,n-1}$, in μ Hz) as a function of the radial order of the modes ($n = 8$ to 29). We subtracted off a linear least squares fit to observational data in order to better display the differences between our calculations and the observations.









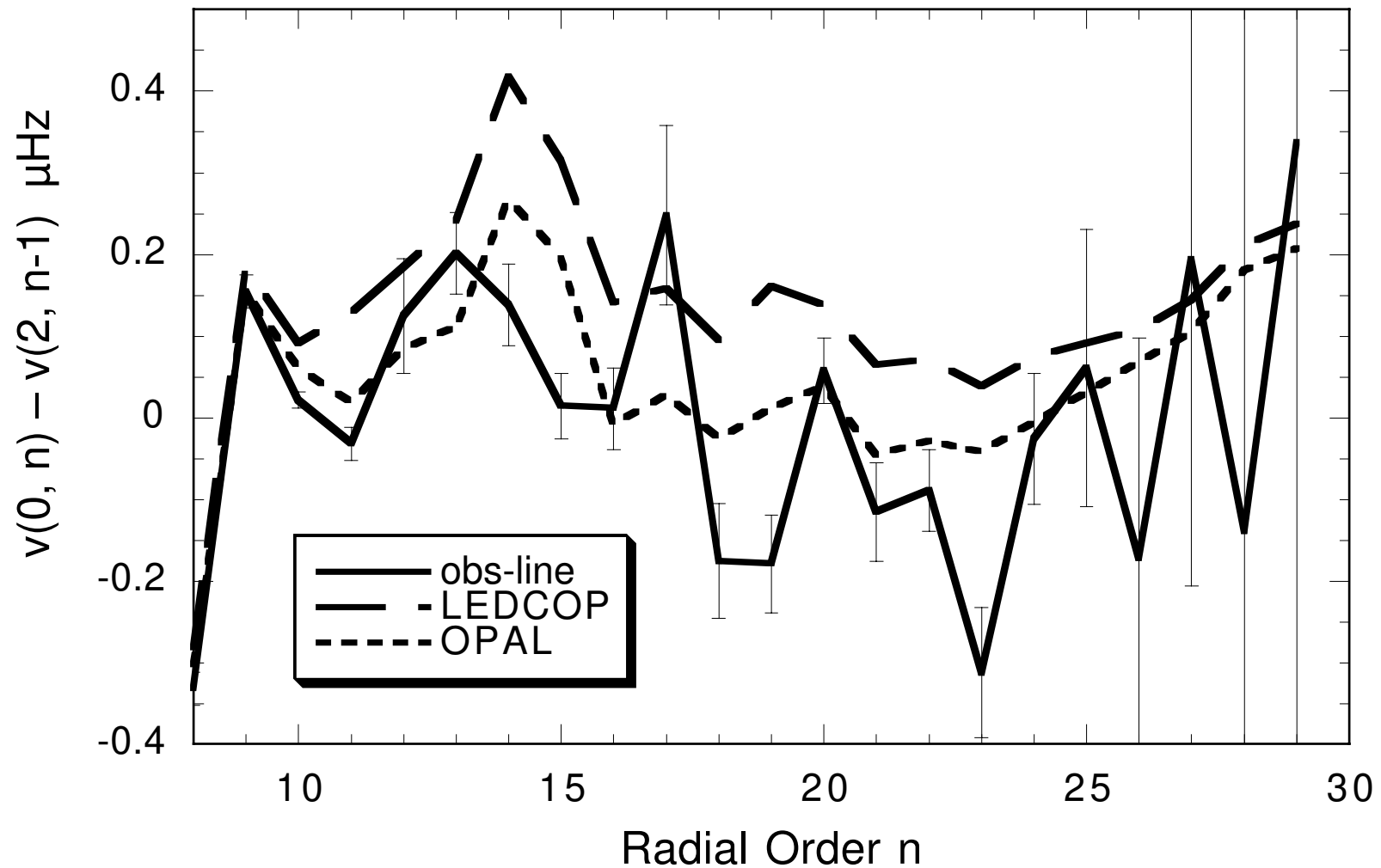


Table 1. Properties of our calibrated models.

Model	OPAL	LEDCOP
X_0	0.7100	0.7122
Y_0	0.2703	0.2680
Z_0	0.0197	0.0198
α	1.7738	1.7651
$\log(L/L_\odot)$	1.9E-04	1.9E-04
$\log(R/R_\odot)$	6.2E-07	6.4e-6
Z/X	0.0245	0.0245
$T_{\text{central}} (10^6 \text{K})$	15.66	15.66
$\rho_{\text{central}} (\text{g/cm}^3)$	152.2	150.8
Y_{central}	0.6375	0.6350
Z_{central}	0.0208	0.0209
$R_{\text{convection zone base}} (R_\odot)$	0.7135	0.7177
$T_{\text{convection zone base}} (10^6 \text{K})$	2.195	2.148
$Y_{\text{convection zone}}$	0.2408	0.2382
^{37}Cl	7.85	7.81
^{71}Ga	128.8	128.2

Note. — X_0 , Y_0 and Z_0 are the initial hydrogen, helium and heavy element mass fraction of our models. α is the convection parameter. All the other quantities are for the present Sun. ^{37}Cl and ^{71}Ga are the predicted event rates for the chlorine and gallium experiments, and are calculated using the neutrino capture cross sections given in Bahcall & Ulrich (1988), Bahcall et al. (1996), and Bahcall (1997). The event rates are expressed in SNUs, one SNU being 10^{-36} interactions per target atom per second.